Spatiotemporal self-similar solutions for the nonautonomous (3+1)-dimensional cubic–quintic Gross–Pitaevskii equation*

Dai Chao-Qing(戴朝卿)†, Chen Rui-Pin(陈瑞品), and Wang Yue-Yue(王悦悦)

School of Sciences, Zhejiang Agricultural and Forestry University, Lin'an 311300, *China*

(Received 24 May 2011; revised manuscript received 2 September 2011)

With the help of similarity transformation, we obtain analytical spatiotemporal self-similar solutions of the nonautonomous (3+1)-dimensional cubic–quintic Gross–Pitaevskii equation with time-dependent diffraction, nonlinearity, harmonic potential and gain or loss when two constraints are satisfied. These constraints between the system parameters hint that self-similar solutions form and transmit stably without the distortion of shape based on the exact balance between the diffraction, nonlinearity and the gain/loss. Based on these analytical results, we investigate the dynamic behaviours in a periodic distributed amplification system.

Keywords: Gross–Pitaevskii equation, similarity transformation, self-similar solutions

PACS: 05.45.Yv, 42.81.Dp **DOI:** 10.1088/1674-1056/21/3/030508

1. Introduction

In the past few decades, the construction of exact solutions for nonlinear partial differential equations (NLPDEs) has made a tremendous amount of progress in mathematics and physics.[1−6] According to previous studies, a vast variety of methods has been developed to obtain exact solutions to a given NLPDE, such as the Jacobian elliptic function method,[1,2] the improved projective approach,[3,4] the mapping method,[5] (G'/G)-expansion method,[6] and the Hirota method.[7]

Among the most important models in modern nonlinear sciences, the nonlinear Schrödinger equation (NLSE) and Gross–Pitaevskii equation (GPE) play important roles in numerous branches of physics, such as nonlinear optics, Bose–Einstein condensates (BECs), plasma physics, and hydrodynamics. The (1+1)-dimensional ((1+1)D) NLSE with distributed coefficients[8−10] has been extensively discussed, but less research work for higher-dimensional NLSE was carried out. Part of the reason may be that all localized solutions are usually unstable for (2+1)D and (3+1)D constant-coefficient NLSE due to weak and strong collapses.[11] However, different situations are found in BECs and nonlinear optics with temporally or spatially modulated parameters. In a variational and numerical treatment, Adhikari[12] has shown that the spatiotemporal optical solitons can be stabilized by a rapidly oscillating scattering length or the dispersion coefficient in a Kerr medium with cubic nonlinearity. Moreover, alteration of the atomic scattering length achieved by Feshbach resonance has been used to dynamically stabilize higher-dimensional bright solitons.[13]

Nowadays, spatiotemporal structures for higher-dimensional NLSE or GPE have flourished into a research area of great importance and interest in many different contexts of nonlinear optics[14,15] and Bose–Einstein condensations (BECs).[16,17] As one of them, solitons stem from the fine balance of diffraction and nonlinearity in various nonlinear systems. Recent progress haa generated novel concepts such as the similariton,[9,14,15] which appears when the coaction of nonlinearity, diffraction and gain in a high-power fiber amplifier causes the shape of an arbitrary input pulse to converge asymptotically to a pulse whose shape is self-similar. In this paper, we will develop a uni-

*Project supported by the National Natural Science Foundations of China (Grant No. 11005092), the Program for Innovative Research Team of Young Teachers (Grant No. 2009RC01), and the Scientific Research and Developed Fund of Zhejiang Agricultural and Forestry University, China (Grant No. 2009FK42).

†Corresponding author. E-mail: dcq424@126.com

© 2012 Chinese Physical Society and IOP Publishing Ltd

fied way to find the similarity transformation for the (3+1)D NLSE or GPE with distributed coefficients. Based on the similarity transformation, we analytically obtain spatiotemporal similaritons and solitons. It is sufficient to mention that these solutions found here depend on the exact balance between different terms in GPE. It is expected that the stability of localized multidimensional solutions will be enhanced in GP systems with oscillating dispersion/diffraction and/or sign-changing nonlinearity.[8,9,14] Finally, we discuss the dynamical behaviours of self-similar solutions.

2. The model and self-similar solutions

We concentrate on the (3+1)D cubic–quintic(CQ) GPE with time–space modulation[18]

$$\mathrm{i}\psi_t + \frac{\beta(t)}{2}\triangle\psi + g_3(t)|\psi|^2\psi + g_5(t)|\psi|^4\psi + V(t)r^2\psi = \mathrm{i}\gamma(t)\psi, \tag{1}$$

where t is time, $\triangle = \partial_x^2 + \partial_y^2 + \partial_z^2$ is the 3D Laplacian, $r^2 = x^2 + y^2 + z^2$, $\psi(t, x, y, z)$ denotes the order parameter with $N = \int |\psi|^2 \mathrm{d}t$ being the number of atoms in the condensate, $g_3(t)$ and $g_5(t)$ are the two-body and three-body attractive (> 0) or repulsive (< 0) interaction functions, $V(t)$ stands for the strength of the harmonic potential. It is strictly assumed that $V \neq 0$; otherwise, we are back to the generalized CQNLSE.[19] The functions $\beta(t)$ and $\gamma(t)$ represent the dispersion/diffraction and gain or loss coefficients, respectively. All coordinates are made dimensionless by the choice of coefficients.

Our first objective is to transform Eq. (1) into a traceable CQNLSE

$$\mathrm{i}\Psi_T + \frac{B}{2}\Psi_{XX} + G_3|\Psi|^2\Psi + G_5|\Psi|^4\Psi = 0, \tag{2}$$

where $T = T(t)$, $X = X(t, x, y, z)$, parameters B, G_3 and G_5 are three real constants. Note that we reduce the (3+1)D CQGPE (1) into the CQNLSE with constant coefficients, which is much more general than the stationary CQNLSE in Ref. [8].

To connect Eq. (1) with Eq. (2), we construct the similarity transformation[14]

$$\psi(t, x, y, z) = \rho(t)\,\mathrm{e}^{\mathrm{i}\varphi(t,x,y,z)}\Psi(T, X). \tag{3}$$

The substitution of Eq. (3) into Eq. (2) leads to Eq. (1), and after some algebra we obtain the following simplest particular solutions for the similarity variable, the width of the pulse, position, amplitude and phase:

$$X = \frac{X_\mathrm{c}}{W(t)} = \frac{\zeta - \zeta_\mathrm{c}(t)}{W(t)}, \quad W(t) = \frac{3Bg_3\exp(2\Gamma)}{\beta}, \tag{4}$$

$$\zeta = k_1x + k_2y + k_3z, \quad \zeta_\mathrm{c}(t) = -9W\int_0^t \frac{B^2\beta(\tau)}{W^2(\tau)}\mathrm{d}\tau, \tag{5}$$

$$A = \frac{\sqrt{\frac{G_3}{B}\left(\sum_{i=1}^3 k_i^2\right)}}{W}\sqrt{\frac{\beta}{g_3}},$$

$$T = \int_0^t \frac{\left(\sum_{i=1}^3 k_i^2\right)\beta(\tau)}{BW^2(\tau)}\mathrm{d}\tau, \tag{6}$$

$$\varphi = \frac{W_t}{2\beta W}r^2 - \frac{3B^2}{W}\left(\frac{x}{k_1} + \frac{y}{k_2} + \frac{z}{k_3}\right) - \frac{9B^4}{2}\left(\sum_{i=1}^3 \frac{1}{k_i^2}\right)\int_0^t \frac{\beta(\tau)}{W^2(\tau)}\mathrm{d}\tau, \tag{7}$$

where $\Gamma(t) = \int_0^t \gamma(\tau)\mathrm{d}\tau$, $k_1 \equiv k$, $k_2 \equiv l$ and $k_3 \equiv m$ are three real constants.

The existence of such solutions should satisfy the following constraints for V and g_5:

$$V = \frac{\beta W_{tt} - \beta_t W_t}{2\beta^2 W}, \quad g_5 = \frac{G_5 B g_3^2 W^2}{G_3^2\left(\sum_{i=1}^3 k_i^2\right)\beta}. \tag{8}$$

Note that the existence of the coefficient $V(t)$ makes the solution of Eq. (1) more difficult than that of the corresponding generalized CQNLSE in Ref. [18]. For vanishing external potential, Eq. (8) hints $W = 1 + s_0\int_0^t \beta\mathrm{d}\tau$. Then the second expression of Eq. (8) is the constraint expressed as Eq. (16) in Ref. [19] when t and z are exchanged here. Also note that the coefficient $\beta(t)$ cannot be zero, otherwise this solution will vanish from Eqs. (4)–(8).

The one-to-one correspondence Eq. (3) admits us to obtain abundant solutions of Eq. (1). Via the similarity transformation Eq. (3), Eq. (1) can be reduced to the constant-coefficient CQNLSE (2). Then by the transformation Eq. (3), we derive the following self-similar solutions:

$$\psi(t, x, y, z) = \rho(t)\sqrt{\lambda \pm \lambda\Theta(\theta, m_0)}\exp\left[\mathrm{i}\phi(t, x, y, z)\right], \tag{9}$$

where $\theta = X - vT$, $\phi(t, x, y, z) = \varphi(t, x, y, z) + pT + vX$ and the function $\Theta(\theta, m_0)$ is one of the Jacobian elliptic functions in Table 1 with modulus m_0 ($0 < m_0 < 1$) describing the degree of the energy localization of waves. Parameters λ and v are arbitrary form-factors, and G_3, G_5 and p related to Jacobian elliptic functions $\Theta(\theta, m_0)$ are shown in Table 1.

Table 1. Jacobian elliptic function solutions.

Solution	G_3	G_5	p	Θ	$m_0 = 0$	$m_0 = 1$
1	$\pm\frac{Bm_0^2}{\lambda}$	$-\frac{3Bm_0^2}{8\lambda^2}$	$\frac{B(1-5m_0^2)}{8} - \frac{v^2}{2B}$	sn	sin	tanh
2	$\mp\frac{Bm_0^2}{\lambda}$	$\frac{3Bm_0^2}{8\lambda^2}$	$\frac{B(4m_0^2+1)}{8} - \frac{v^2}{2B}$	cn	cos	sech
3	$\mp\frac{B}{\lambda}$	$\frac{3B}{8\lambda^2}$	$\frac{B(4+m_0^2)}{8} - \frac{v^2}{2B}$	dn	1	sech
4	$\pm\frac{B}{\lambda}$	$-\frac{3B}{8\lambda^2}$	$\frac{B(m_0^2-5)}{8} - \frac{v^2}{2B}$	ns	csc	coth
5	$\mp\frac{B(m_0^2-1)}{\lambda}$	$\frac{3B(m_0^2-1)}{8\lambda^2}$	$\frac{B(4m_0^2-5)}{8} - \frac{v^2}{2B}$	nc	sec	cosh
6	$\mp\frac{B(m_0^2-1)}{\lambda}$	$\frac{3B(1-m_0^2)}{8\lambda^2}$	$\frac{B(4-5m_0^2)}{8} - \frac{v^2}{2B}$	nd	1	cosh
7	$\pm\frac{Bm_0^2}{\lambda}$	$-\frac{3Bm_0^2}{8\lambda^2}$	$\frac{B(1-5m_0^2)}{8} - \frac{v^2}{2B}$	cd	cos	1
8	$\pm\frac{B}{\lambda}$	$-\frac{3B}{8\lambda^2}$	$\frac{B(m_0^2-5)}{8} - \frac{v^2}{4B}$	dc	sec	1

3. Periodic behaviours for self-similar solutions

In what follows, we will focus on the periodic varying diffraction and nonlinear parameters[20] $\beta(t) = \beta_0[1+\epsilon_1\sin(\kappa t)]$, $\chi(t) = \chi_0[1+\epsilon_2\sin(\kappa t)]$ and a small constant gain/loss parameter $\gamma(t) = \gamma_0$. In practice, the modulations of β and χ depend on the use of the optical lattice and Feshbach-resonance techniques by exerting particular time-dependent optical field and magnetic field.

The dynamics of the spatiotemporal self-similar solutions are exhibited in Figs. 1–5. Similar to the specific soliton management,[7,13,19] the similariton dynamics can also be controlled by the corresponding management functions. From these spatiotemporal scenarios of the density distributions $I = |\psi|^2$ shown in Figs. 1–4, we find the novel reversal phenomenon of gain and loss. For the loss case $\gamma = -0.01$, the intensity of self-similar cnoidal waves and similaritons is enhanced. For the gain case $\gamma = 0.01$, the intensity of self-similar cnoidal waves and similaritons attenuates instead. The reason to generate this phenomenon is the appearance of the width function $W(t)$ in the amplitude, as seen from Eqs. (4) and (6). Note that an important feature which distinguishes our solutions from the others reported in Ref. [18] is the universal influence of the width function $W(t)$ on the solutions of all other parameters, which generates the novel reversal phenomenon of gain and loss. The width function $W(t)$ influences not only the form of the amplitude, the phase and the position, but also the curvature of the wave-front, the frequency shift and the homogeneous phase shift. Quantitatively, from solution (9) together with Eqs. (4)–(7), we can see that the velocity of self-similar waves is determined by $[9B^2 - v(\sum_{i=1}^{3} k_i^2)/B]\beta(t)/W^2(t)$, the chirps are both related to $W_t/[2\beta(t)W(t)]$, the time shifts are both described by $[9B^2 - v(\sum_{i=1}^{3} k_i^2)/B]\int_0^t \frac{\beta(\tau)}{W^2(\tau)}\mathrm{d}\tau$, and the amplitudes are both determined by $\frac{\sqrt{\frac{G_3}{B}\left(\sum_{i=1}^{3} k_i^2\right)}}{W}\sqrt{\frac{\beta}{g_3}}$. Therefore, we can select the system parameters $\beta(t)$, $\gamma(t)$ and $g_3(t)$ to control the formation of self-similar waves.

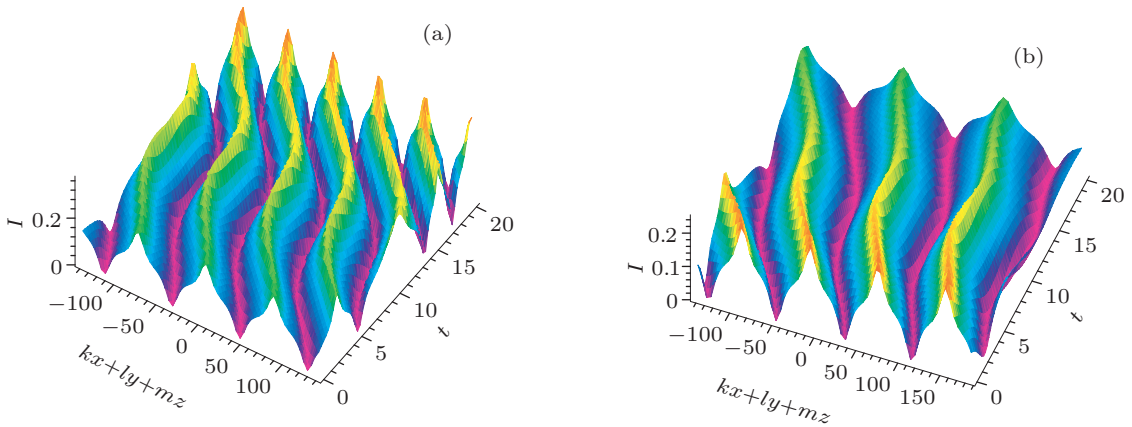


Fig. 1. (colour online) Evolutions of a self-similar cn-wave with $\Theta(\theta, m_0) = \mathrm{cn}(\theta, m_0)$ in the "+"-branch of Eq. (9) with (a) the loss coefficient $\gamma_0 = -0.01$ and (b) the gain coefficient $\gamma_0 = 0.01$.

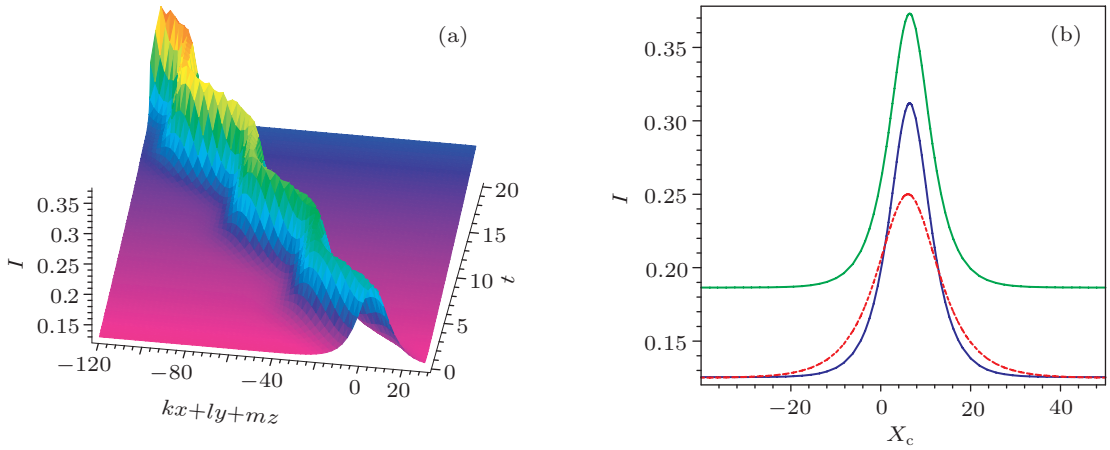


Fig. 2. (colour online) (a) Evolution of a bright similariton corresponding to Fig. 1(a). (b) The corresponding sectional view. Here, the red dashed line denotes the initial wave, the green line is the wave at time $t = 20$, and the blue line is the translational line corresponding to the green line.

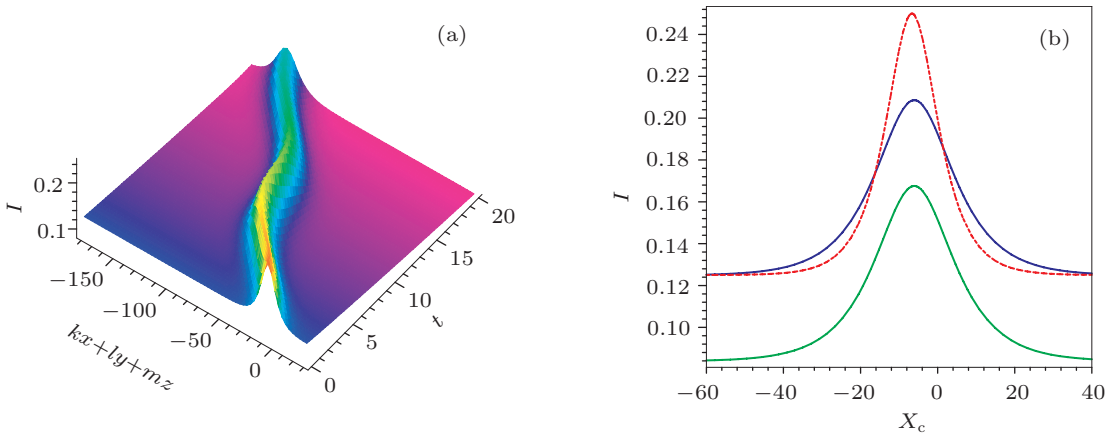


Fig. 3. (colour online) (a) Evolution of bright similariton corresponding to Fig. 1(b). (b) The corresponding sectional view. Here, the red dashed line denotes the initial wave, the green line is the wave at time $t = 20$, and the blue line is the translational line corresponding to the green line.

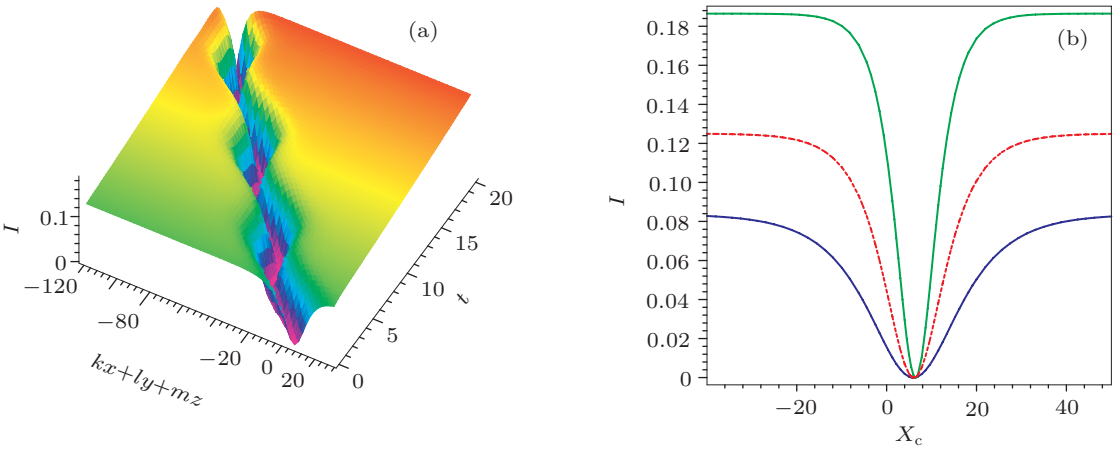


Fig. 4. (colour online) (a) Evolutions of dark similariton with $\Theta(\theta) = \mathrm{sech}(\theta)$ in the "−"-branch of Eq. (9) with the loss coefficient $\gamma_0 = -0.01$. (b) The corresponding sectional view. Here, the red dash line denotes the initial wave, the green line is the pulse for the loss case at time $t = 20$, and the blue line represents the wave for the gain case at time $t = 20$. The other parameters are the same as those in Fig. 1.

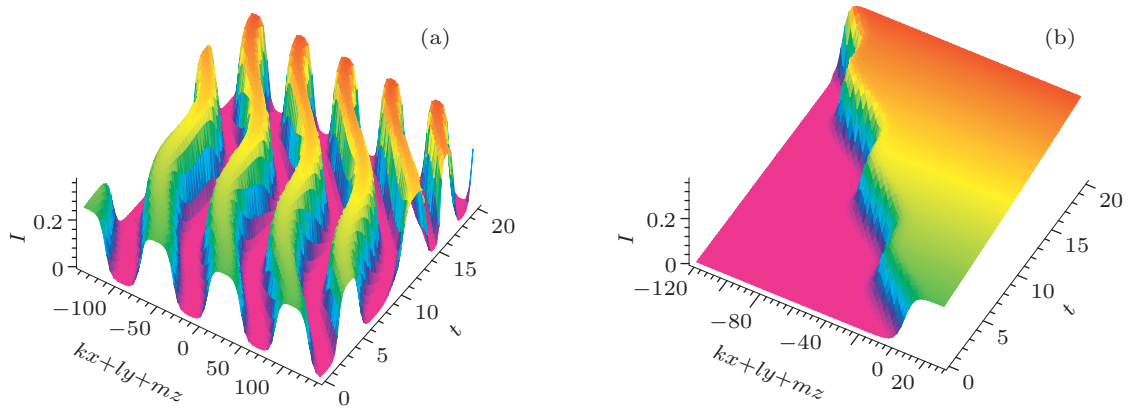


Fig. 5. (colour online) (a) Evolutions of a self-similar sn-wave with $\Theta(\theta, m_0) = \mathrm{sn}(\theta, m_0)$ in the "+"-branch of Eq. (9) with the loss coefficient $\gamma_0 = -0.01$. (b) The corresponding kink similariton. The other parameters are the same as those in Fig. 1.

From Fig. 1, the period in space of the loss case (Fig. 1(a)) is smaller than that of the gain case (Fig. 1(b)), that is, in the same space interval the wave number for the loss case is bigger than that of the gain case. Here, the parameters are taken as $\epsilon_1 = \epsilon_2 = 0.8$, $\beta_0 = \chi_0 = G_3 = k_1 = k_3 = 1$, $\lambda = \kappa = v = 0.5$, $B = k_2 = 2$, and $m_0 = 0.99$. The corresponding bright similaritons for Fig. 1 are shown in Figs. 2 and 3. From Fig. 2(b), the similariton is compressed, namely the width decreases and the amplitude increases. For Fig. 3(b), the similariton is stretched, namely the width increases and the amplitude reduces. Here, the red dash line denotes the initial pulse, the green line is the pulse at time $t = 20$, and the blue line is the translational line corresponding to the green line for comparing the final pulse with the initial pulse. The study shows that the propagation behaviours of dark similaritons have similar behaviours to that of bright similaritons in Figs. 2 and 3. Figure 4 indicates that the pulse is compressed for the loss case while extended for the gain case. The red dashed line denotes the initial pulse, the green line is the pulse for the loss case at time $t = 20$, and the blue line represents the pulse for the gain case at time $t = 20$. Figure 5 displays the periodic behaviour of a self-similar sn-wave and the corresponding kink similariton. Their evolutional behaviours are similar to cn-waves, bright and dark similaritons in Figs. 1–4, i.e., the intensity of self-similar sn-waves are enhanced for the loss case, while they attenuate for the gain case.

4. Conclusions

In conclusion, first we analytically obtained self-similar solutions of the nonautonomous (3+1)D GPE with time-dependent diffraction, nonlinearity, harmonic potential and gain or loss. Then we looked at the periodic distributed diffraction and nonlinearity with constant gain case to analyse the dynamics of self-similar solutions. The influence of the width function on the position, the phase and the amplitude of solutions is elucidated, and it generates a novel reversal phenomenon of gain and loss, that is, the intensity of self-similar solutions enhances for the loss case, while it attenuates for the gain case. It is also shown that the pulse can be compressed or extended to a desired width and amplitude in a controllable manner by the choice of gain/loss parameter. We expect that experimental investigation on the predictions of this paper will be performed in future.

References

[1] Dai C Q and Zhang J F 2005 *Int. Mod. Phys.* B **19** 2129
[2] Liu S K, Zhao Q and Liu S D 2011 *Chin. Phys.* B **20** 040202
[3] Yang Z, Ma S H and Fang J P 2011 *Chin. Phys.* B **20** 040301
[4] Yang Z, Ma S H and Fang J P 2011 *Chin. Phys.* B **20** 060506
[5] Dai C Q and Zhang J F 2006 *Opt. Commun.* **263** 309
[6] Li B Q, Ma Y L, Wang C, Xu M P and Li Y 2011 *Acta Phys. Sin.* **60** 060203 (in Chinese)
[7] Wang H and Li B 2011 *Chin. Phys.* B **20** 040203
[8] Qian C, Wang L L and Zhang J F 2011 *Acta Phys. Sin.* **60** 064214 (in Chinese)
[9] Dai C Q, Wang Y Y and Yan C J 2010 *Opt. Commun.* **283** 1489
[10] Zong F D, Yang Y and Zhang J F 2011 *Acta Phys. Sin.* **60** 3670 (in Chinese)
[11] Sulem C and Sulem P 2000 *The Nonlinear Schrödinger Equation: Self-Focusing and Wave Collapse* (Berlin: Springer-Verlag)
[12] Adhikari S K 2004 *Phys. Rev.* A **69** 063613
[13] Saito H and Ueda M 2003 *Phys. Rev. Lett.* **90** 040403

[14] Dai C Q, Wang Y Y and Zhang J F 2010 *Opt. Lett.* **35** 1437

[15] Dai C Q, Chen R P and Zhou G Q 2011 *J. Phys.* B: *At. Mol. Opt. Phys.* **44** 145401

[16] Dai C Q, Wang D S, Wang L L, Zhang J F and Liu W M 2011 *Ann. Phys.* **326** 2356

[17] Zhang W X, She Y C and Wang D L 2011 *Acta Phys. Sin.* **60** 070514 (in Chinese)

[18] Abdullaev F K, Gammal A, Tomio L and Frederico T 2001 *Phys. Rev.* A **63** 043604

[19] Jiang L H and Wu H Y 2011 *Opt. Commun.* **284** 2022

[20] Yang R C, Hao R Y, Li L, Shi X J, Li Z H and Zhou G S 2005 *Opt. Commun.* **253** 177